Available online at www.sciencedirect.com
SCIENCE DIRECT®
ELSEVIER
Nuclear Instruments and Methods in Physics Research B 230 (2005) 148–157
NIM B
Beam Interactions with Materials & Atoms
www.elsevier.com/locate/nimb

Energy loss of ions interacting with metal surfaces

J.I. Juaristi *

Departamento de Física de Materiales y Unidad de Física de Materiales Centro Mixto CSIC-UPV/EHU, Facultad de Químicas, UPV/EHU, Apdo. 1072, 20018 San Sebastián, Spain

Available online 21 January 2005

Abstract

The problem of calculating the energy loss of ions specularly reflected by metal surfaces is treated. Different approximations for the treatment of the screening and scattering are presented and their validity in the different coupling regimes is discussed. Illustrative comparisons with available experiments are provided.

PACS: 34.50.Bw; 34.50.Dy
Keywords: Stopping power; Ion; Surface; Metals

1. Introduction

The study of the energy loss of atomic particles scattered off metal surfaces constitutes an active field of research [1–12]. If one wants to obtain information on surface related properties the trajectories of interest are those for which the particle interacts during a long time with the metal surface before it is reflected. This situation is achieved by using projectiles with small energy in the normal direction, as it is the case in grazing ion surface collisions [1]. The aim of this work is to review some recent developments on this problem, focusing on the theoretical approaches that have been used to characterize and understand the energy loss mechanisms under these conditions.

For specularly reflected ions under grazing angle of incidence one can calculate the total energy loss ΔE in the following way [5]:

$$\Delta E = 2v \int_{z_{tp}}^{\infty} S(z) \frac{1}{v_z(z)} \, dz, \tag{1}$$

where v is the velocity of the projectile, $v_z(z)$ is the component of v normal to the surface, z_{tp} is the turning point of the trajectory and $S(z)$ is the so-called distance dependent stopping power, i.e. the energy lost per unit path length traveled by the ion parallel to the surface as a function of the ion-surface separation z. Since the total energy loss in a typical trajectory amounts just a few

* Tel.: +34 943 015396; fax: +34 943 015270.
E-mail address: wapjuoli@sq.ehu.es

0168-583X/$ - see front matter
doi:10.1016/j.nimb.2004.12.033

percent of the initial one, v is taken as a constant. The knowledge of $v_z(z)$ requires a calculation of the trajectory. Finally $S(z)$ is the central quantity in the study of the energy loss of ions under grazing incidence.

Different approximations for the calculation of $S(z)$ have been used. In the weak coupling regime $Z_1/v \ll 1$, where Z_1 is the charge of the projectile, linear response theory can be used to describe the screening and the energy loss of the projectile. In Section 2 the main features of linear response theory as applied to this problem are discussed. Comparison with experiments for the case of 710 keV protons scattered off Al(1 1 1) is provided. In the strong coupling regime ($Z_1/v \gg 1, v < v_F$), where v_F is the Fermi velocity of the metal electrons, the projectile represents a strong perturbation and linear response theory is not valid. In this case, density functional theory (DFT) to calculate the induced screened potential, together with a full phase-shift calculation of the cross-sections, has successfully described the stopping power and energy loss of slow ion projectiles in the bulk of metals. In Section 3 it is shown how this formalism has helped to understand experiments in which slow ion projectiles were scattered off metal surfaces. Finally, a brief summary is given in Section 4.

The common feature of the theoretical approaches presented here is the use of the free electron gas model. In this model the only parameter used is the mean electronic density of the system n_0. In this respect, it is customary to use the one-electron radius r_s, defined as $1/n_0 = 4/3\pi r_s^3$. Atomic units (a.u.) will be used unless it is otherwise stated.

2. High velocities: linear response theory

2.1. Model

When a swift charged particle interacts with matter, it induces a polarization potential $V^{\text{ind}}(\mathbf{r}, t)$. This potential acts back on the projectile giving rise to a retarding force. The energy that the particle loses per unit time due to this force, can be calculated in the following way:

$$\frac{dE}{dt} = -\int d\mathbf{r}\rho^{\text{ext}}(\mathbf{r}, t)\frac{\partial V^{\text{ind}}(\mathbf{r}, t)}{\partial t}, \tag{2}$$

where $\rho^{\text{ext}}(\mathbf{r}, t)$ represents the probe-particle charge density.

Henceforth, z is the coordinate of the position vector normal to the surface. The topmost atomic layer is at $z = 0$ and the solid is in the $z < 0$ side. Capital letters are used for the coordinates parallel to the surface ($\mathbf{r} = (\mathbf{R}, z)$). Here, it is studied the case of a point charge Z_1 moving parallel to the surface with velocity $\mathbf{v}$ at a distance $z_0 > 0$:

$$\rho^{\text{ext}}(\mathbf{r}, t) = Z_1\delta(\mathbf{R} - \mathbf{v}t)\delta(z - z_0). \tag{3}$$

Translational invariance in the plane parallel to the surface is assumed, i.e. surface corrugation effects are neglected. This is a reasonable approximation considering that only ions incident under random directions are considered. In this case, within linear response theory, the potential induced by an external charge can be calculated in terms of the two dimensional Fourier transform of the induced part of the screened interaction $W^{\text{ind}}(Q, z, z', \omega)$ [13]:

$$V^{\text{ind}}(\mathbf{r}, t) = \int \frac{d^2\mathbf{Q}}{(2\pi)^2}\int \frac{d\omega}{2\pi} e^{i(\mathbf{Q}\cdot\mathbf{R} - \omega t)} \times \int dz' W^{\text{ind}}(Q, z, z', \omega)\rho^{\text{ext}}(Q, z', \omega), \tag{4}$$

where $\rho^{\text{ext}}(Q, z, \omega) = 2\pi Z_1\,\delta(\omega - \mathbf{Q}\cdot\mathbf{v})\,\delta(z - z_0)$ is the Fourier transform of the external charge density of Eq. (3) with respect to $\mathbf{R}$ and t.

Substituting Eq. (4) in Eq. (2) and making use of the parity properties of $W^{\text{ind}}(Q, z, z', \omega)$, one can write the above defined distance dependent stopping power $S(z_0)$ in the following way [6,11]:

$$S(z_0) = \frac{1}{v}\frac{dE}{dt} = \frac{-2Z_1^2}{v}\int \frac{d^2\mathbf{Q}}{(2\pi)^2}\mathbf{Q}\cdot\mathbf{v} \times \mathrm{Im}\{W^{\text{ind}}(Q, z_0, z_0, \mathbf{Q}\cdot\mathbf{v})\}\Theta(\mathbf{Q}\cdot\mathbf{v}), \tag{5}$$

where $\Theta(x)$ is the Heaviside step function.

$W^{\text{ind}}(Q, z, z', \omega)$ has a rigorous expression in terms of the exact density-density correlation function of the system $\chi(Q, z, z', \omega)$ [6]:

$$W^{\mathrm{ind}}(Q,z,z',\omega) = \left(\frac{2\pi}{Q}\right)^2 \int \mathrm{d}z_1 \int \mathrm{d}z_2 \mathrm{e}^{-Q(|z_1-z|+|z_2-z'|)}\chi(Q,z_1,z_2,\omega). \quad (6)$$

In general, $\chi(Q,z,z',\omega)$ is a very complex function, being hard to calculate it exactly. Here, the random phase approximation (RPA) is used, that allows one to write $\chi(Q,z,z',\omega)$ in terms of the density response function for noninteracting electrons, $\chi_0(Q,z,z',\omega)$ as [14,15]

$$\chi(Q,z,z',\omega) = \chi_0(Q,z,z',\omega) + \int \mathrm{d}z_1 \int \mathrm{d}z_2 \chi_0(Q,z,z_1,\omega) \times V_{\mathrm{ee}}(Q,z_1,z_2)\chi(Q,z_2,z',\omega), \quad (7)$$

where the electron–electron interaction potential is $V_{\mathrm{ee}}(Q,z_1,z_2) = (2\pi/Q)\mathrm{e}^{-Q|z_1-z_2|}$. Though the inclusion of local field corrections to $V_{\mathrm{ee}}(Q,z_1,z_2)$ constitutes an improvement over the RPA response function, their effect in $S(z_0)$ is almost negligible [11], and therefore they are not considered here.

With $\Psi_i \sim e^{i\mathbf{Q}'\cdot R}\phi_i(z)$ and $E_i = Q'^2/2 + \varepsilon_i$ as the one-electron wave functions and eigenvalues of the one-electron Hamiltonian, the density response function $\chi_0(Q,z,z',\omega)$ can be written in the following way [14,15]:

$$\chi_0(Q,z,z',\omega) = 2\sum_{i,j} \phi_i(z)\phi_j^*(z)\phi_j(z')\phi_i^*(z') \times \int \frac{\mathrm{d}\mathbf{Q}'}{(2\pi)^2} \frac{\Theta(E_{\mathrm{F}}-E_i)-\Theta(E_{\mathrm{F}}-E_j)}{E_i-E_j+(\omega+\mathrm{i}\eta)}, \quad (8)$$

where η is a positive infinitesimal, $E_j = (\mathbf{Q}'+\mathbf{Q})^2/2 + \varepsilon_j$ and E_{F} is the Fermi energy of the system.

A successful description of the electronic properties of the surface, and therefore of the one-electron wave functions and energies entering the calculation of $\chi_0(Q,z,z',\omega)$ is based on the jellium model. The ionic background made up of nuclei and core electrons is replaced by a uniform positive charge distribution that extends up to $z = d/2$, where d is the interplanar separation in the direction normal to the surface. From now on, the distance $z = d/2$ will be called the jellium edge. Using the potential created by this distribution of charge as input external potential, one calculates self-consistently, using density functional theory (DFT) within the Kohn–Sham (KS) formalism, a finite and smooth surface potential barrier and the corresponding KS wave functions and eigenvalues. These KS wave functions and eigenvalues are the ones that are used in the calculation of $\chi_0(Q,z,z',\omega)$. In the following I will refer to this model as jellium model.

A much more simple model, and computationally less exigent, that has been widely used is the so-called specular reflection model (SRM) [16,17]. This approximation consists in assuming that the conduction electrons are confined by an infinite barrier potential (located at the jellium edge), and in neglecting the quantum interference between the outgoing and ingoing components of the wave functions of the electrons reflected at this barrier. This approximation makes straightforward to obtain $W^{\mathrm{ind}}(Q,z,z',\omega)$ from the knowledge of the bulk dielectric function $\epsilon(k,\omega)$. Explicit expressions can be found in [13].

In the following, the results obtained with the jellium model and the SRM are compared. In the SRM, the Lindhard random phase approximation [18] has been used for the bulk dielectric function. Fig. 1 show the results obtained for $S(z_0)$ the stopping power for a proton travelling parallel to an Al(1 1 1) surface with velocities $v = 0.5$ a.u. and $v = 4$ a.u., respectively. Within these models, the Al (1 1 1) surface is described by taking $r_{\mathrm{s}} = 2.07$ as the radius per electron in the conduction band and locating the jellium edge at $z = 2.21$ a.u. from the topmost layer. Though for $v = 0.5$ a.u. one is out of the range of applicability of linear response theory, these results are shown in order to get a physical insight on the differences between the two models. In all the cases, well inside the solid, all the models results tend to the corresponding value of the bulk electronic stopping power. At low velocities, the SRM underestimates the value of the stopping at large distances, because in this model the induced charge is confined to the surface by the infinite potential barrier. Nevertheless, at high velocities SRM shows to be a good approximation for the more realistic jellium model. The reason for this is that in this velocity range the energy loss at large distances from the surface is governed by small momentum transfer excitations such as surface plasmons. Their description does not almost depend on the details of the surface

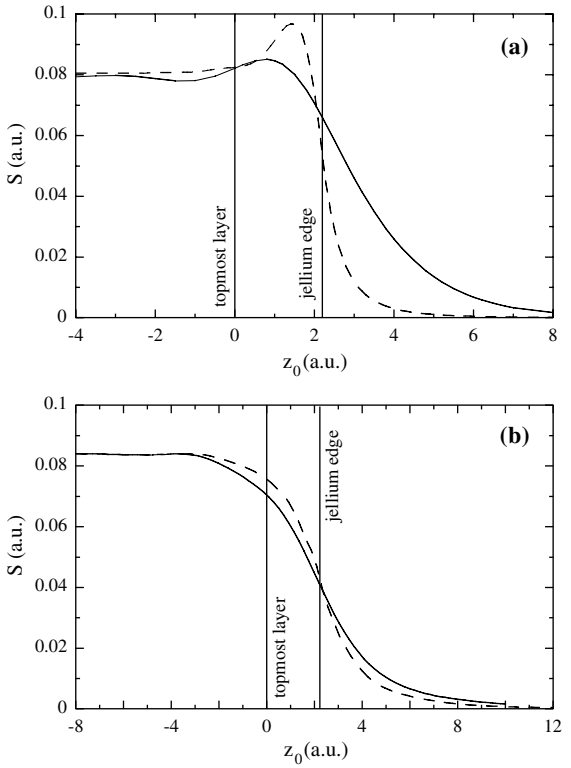

Fig. 1. Stopping power S of a proton travelling parallel to an Al(1 1 1) surface as a function of its distance to the topmost layer z_0, calculated within the jellium model (solid line) and the SRM (dashed line). The position of the jellium edge for this surface is located at $z_0 = 2.21$ a.u. In figure (a) the velocity of the proton is $v = 0.5$ a.u. and in figure (b) $v = 4$ a.u.

potential. More precisely, the SRM provides a good description of the plasmon excitations, and therefore it is a valuable approximation for the energy loss of high velocity projectiles.

Finally, it is worth mentioning that recently some calculations of $S(z_0)$ have been performed without invoking the jellium model and using information about the surface band structure of the solid [19,20]. Calculations for the Cu(1 1 1) surface were performed. The Cu(1 1 1) surface exhibits a band gap of around 5 eV and presents a surface state located in energy just above the bottom of the band gap. It was shown that the results for $S(z_0)$ did not differ so much from those obtained within the jellium model. Briefly, the presence of the surface state compensates the reduction of the stopping due to the surface band gap.

2.2. Energy loss of fast protons scattered off Al(1 1 1)

As an application of the approach presented above results are presented for the energy loss of 710 keV protons scattered off Al(1 1 1). In this way one can compare the theoretical results with available experimental data [21]. Note that for the high velocities under consideration, in addition to the valence band excitations, one has to consider that the projectile can also excite electrons in the inner-shells of the target atoms. This contribution to the energy loss can be obtained in terms of the impact-parameter dependent energy loss in single encounters of the external charge with the target atoms, which is calculated within first-order Born approximation [22]. In order to obtain the contribution of this channel to the stopping power '$S_{\text{in-sh}}$' an average over the trajectory is performed. See [5] for details.

As an example, Fig. 2 shows the results obtained for S in the case of 710 keV protons ($v = 5.33$ a.u.) as a function of the distance from the Al(1 1 1) surface. The different contributions to the stopping power (valence band and inner-shell excitations) and the total sum are plotted. In the inner-shell contribution only the L-shell of Al has been considered since the K-shell is too strongly bound to be efficiently excited by protons of this energy. It is important to stress the different behaviour with the distance of the contribution of valence band

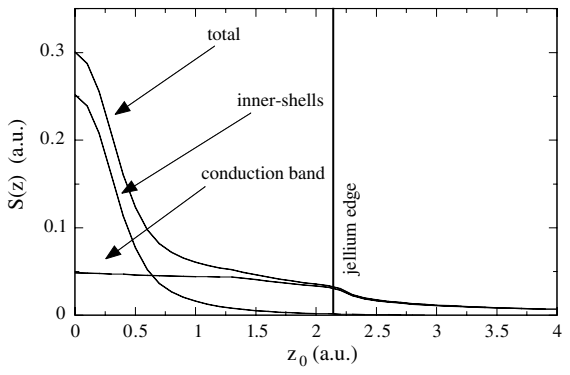

Fig. 2. Stopping power of a 710 keV proton travelling parallel to an Al(1 1 1) surface as a function of its distance to the topmost layer z_0. The contributions of the valence band excitations and inner-shells excitations are distinguished.

excitation, S_{val}, as compared to $S_{in\text{-}sh}$. On the one hand, the latter takes significant values at small distances from the topmost layer of the order of 0.5–1 a.u., where it dominates over the valence band contribution in the range of energies under consideration. On the other hand, S_{val} is important upto distances of the order of the jellium edge position. Consequently, the valence band contribution dominates over the inner-shell contribution except very close to the atomic surface.

In order to compare the theoretical predictions with experimentally measured energy losses it is necessary to evaluate Eq. (1). Therefore, one needs to perform the calculation of the trajectory of the ion under the combined influence of the repulsive surface atomic planar potential and the attractive image potential. In the results presented here, the planar potential is calculated by taking a planar average of the interatomic universal Ziegler–Biersack–Littmark potential [23]. The image potential, calculated as one half of the induced potential at the position of the ion, can be obtained within any of the prescriptions for the induced potential given above. Due to the high velocities under consideration SRM has been used in the calculation of both the image potential and S_{val}.

Fig. 3 shows different contributions to the total energy loss ΔE as a function of the scattering angle (twice the incident angle for specularly reflected particles) for 710 keV protons. It is observed that, at the same time as the contribution of valence band excitations decreases, the contribution due to inner-shell excitations increases when increasing the angle of incidence. The reason for this can be easily understood from the dependence of both S_{val} and $S_{in\text{-}sh}$ on the distance to the surface.

First, let us concentrate on the contribution of conduction band excitations to the energy loss. In Fig. 4 it is shown (in the lower pannel) the trajectory of a 710 keV proton with angle of incidence $\phi = 0.3°$, and (in the upper pannel) the energy loss overcome by the proton upto the corresponding point of the trajectory. It is observed that most of

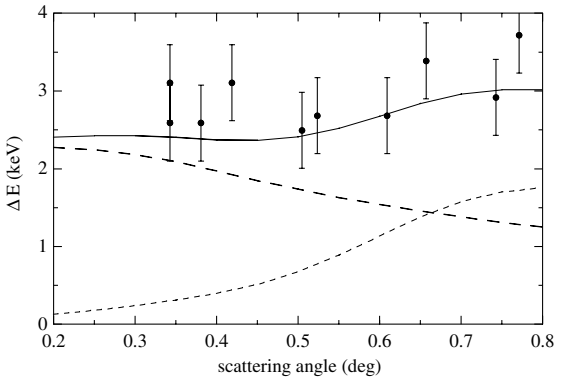

Fig. 3. Energy loss of 710 keV protons specularly reflected at an Al (1 1 1) surface as a function of the scattering angle (solid line). The contributions of the valence band excitations (dashed line) and inner-shell excitations (dotted line) are shown separately. The results are compared to the experimental data of [21].

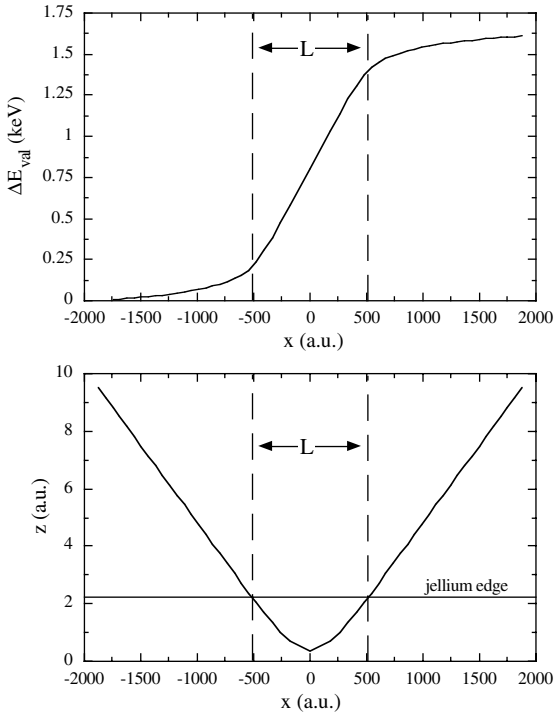

Fig. 4. In the lower pannel it is shown the trajectory for a 710 keV proton specularly reflected from an Al(1 1 1) surface with angle of incidence $\phi = 0.3°$. z and x are the coordinates perpendicular and parallel to the surface, respectively. Note the difference in the scales. The quantity L, defined as the length that the ion travels inside the jellium edge, is also shown. In the upper pannel it is plotted the energy lost by the proton up to the corresponding point of the trajectory (given by the value of the coordinate x) in the excitation of conduction band electrons (ΔE_{val}). It is observed that most of the energy loss takes place inside the jellium edge.

the energy loss takes place inside the jellium edge. Incidentally, this may allow one to define an interaction length (L) as the distance the projectile travels inside this region. The reason for this behaviour is the slow variation of S_{val} within this region. Increasing the angle of incidence results in a reduction of L, with the subsequent reduction of the energy loss due to the excitation of conduction band electrons.

On the contrary, the inner-shell contribution becomes relevant only when the turning point is very close to the atomic surface, where $S_{\text{in-sh}}$ takes appreciable values. The turning point is closer to the atomic surface for larger angles of incidence, and therefore this contribution increases with the angle of incidence. The sum of both contributions, i.e. the total energy loss ΔE, varies smoothly in the range 2–3 keV as a function of the angle of incidence. In Fig. 3, the experimental results obtained by Winter et al. for 710 keV protons [21] are also shown. The agreement obtained between the theoretical and experimental results is remarkable. Moreover, this theoretical approach is able to reproduce the main features found in the fast proton-surface scattering experiments: The smooth dependence of the total energy loss with the initial energy and angle of the projectile [21,24].

3. Slow projectiles: nonlinear theory

3.1. Theory

In the strong coupling regime ($Z_1/v \gg 1$) the projectile represents a strong perturbation for the system and linear response theory is not longer valid. The piling-up of charge in the vicinity of the ion, particularly in the spatial region within a few atomic units around the nucleus, requires a nonlinear description of the electronic density modification [25,26].

The energy loss of slow charges in an electron gas has been widely studied from the theoretical point of view [27–30]. It has been shown that the description of the scattering process by the first Born approximation is not fully satisfactory for slow ions at metallic densities. This is true even for a proton. The use of scattering theory to calculate the cross-sections from the phase shifts allows, in principle, to obtain a result which is valid to all orders in the projectile charge. This approach requires a nonlinear calculation of the self-consistent scattering potential for arbitrary charge Z_1.

In this respect, density functional theory (DFT) has been successfully used in the description of the nonlinear screening effects associated with the interaction of slow ions with metals [31–34]. The starting point is the DFT formalism as applied to a static impurity of charge Z_1 embedded in a free electron gas of mean density n_0 [25,26]. The static approximation is appropriate for ion velocities well below the Bohr velocity [35,36]. In practice, one uses the Kohn–Sham (KS) scheme and obtains the electronic density $n(r)$ as a sum over the occupied single-particle states which are calculated by solving self-consistently the one-electron KS equations. This sum includes a contribution originating from the occupied bound states and another one coming from the integration over the continuum up to the Fermi level. In this way, KS equations allow one to determine the perturbed potential created by the ion and the electronic density around it.

Using the KS potential as scattering potential, the stopping power can be written in terms of the transport cross-section at the Fermi level $\sigma_{\mathrm{T}}(k_{\mathrm{F}})$ as [31]:

$$S = n_0 v k_{\mathrm{F}} \sigma_{\mathrm{T}}(k_{\mathrm{F}}) = Qv, \tag{9}$$

where $Q = n_0 k_{\mathrm{F}} \sigma_{\mathrm{T}}(k_{\mathrm{F}})$ is the so-called friction coefficient, k_{F} is the Fermi momentum, the transport cross-section $\sigma_{\mathrm{T}}(k_{\mathrm{F}})$ is calculated from

$$\sigma_{\mathrm{T}}(k_{\mathrm{F}}) = \frac{4\pi}{k_{\mathrm{F}}^2} \sum_l (l+1) \sin^2[\delta_l(k_{\mathrm{F}}) - \delta_{l+1}(k_{\mathrm{F}})] \tag{10}$$

and $\delta_l(k_{\mathrm{F}})$ are the scattering phase shifts at the Fermi level for electron scattering off the self-consistent screened potential. In Eq. (9) the product $k_{\mathrm{F}}\sigma_{\mathrm{T}}(k_{\mathrm{F}})$ is the integrated scattering rate for momentum transfer, which governs the dissipative process. Therefore, one can interpret the stopping power described by this formula as the result of the momentum transfer per unit time to a uniform current of independent electrons ($n_0 v$) scattered by a fixed screened potential.

3.2. Z_1 oscillations in the energy loss of slow ions interacting with metal surfaces

One of the advantages of this approach is that it allows to understand in a straightforward manner the so-called Z_1 oscillations, an experimentally observed oscillatory behaviour of the stopping power with increasing projectile atomic number Z_1 for ions travelling through metals [37–42]. In this respect, recently, quantitative agreement between theory and experiment has been obtained by measuring the energy loss of ions with atomic number $1 \leqslant Z_1 \leqslant 20$ and velocity $v = 0.5$ a.u. scattered off an Al(1 1 1) surface under grazing angle of incidence [43]. Performing a detailed analysis of the trajectory it is possible to obtain from these experiments the distance dependent stopping power $S(z)$. Eq. (9) is derived for an ion travelling through jellium, and it is expected to be valid for ions travelling through uniform electronic density regions. In case of a surface experiment the ions travel through a region of varying electron density. In order to obtain a position dependent stopping power the natural way to proceed is the following. First, one calculates the electronic density profile at the Al(1 1 1) surface $n_0(z)$. Then, at each distance z, one defines a local Fermi momentum $k_F(z) = \sqrt[3]{3\pi^2 n_0(z)}$ and introduces it in Eq. (9) to obtain $S(z)$.

In Fig. 5 the experimental stopping power at $z = 1.2$ a.u. is compared to the theoretical value of the stopping power. At this distance the corresponding density parameter is $r_s = 2.2$ a.u. The figure shows an excellent quantitative agreement between theory and experiment. Note that at $z = 1.2$ a.u. the electronic density is very close to the bulk value. In this case, effects due to the nonuniformity of the electronic density seem to be negligible, and Eq. (9), valid for uniform systems, is applicable.

Finally, it is worth to mention that this local approach is not successful to account for the experimentally obtained stopping power at larger distances from the surface, where the density gradients due to the nonuniformity of the density profile are comparable (or larger) that the actual value of the density. This can be easily understood, since by construction, the model for the stopping used assumes a medium with uniform electronic density. Nevertheless, as shown in Fig. 5 it represents a good approximation for the stopping power at small distances from the surface, where most of the energy loss takes place.

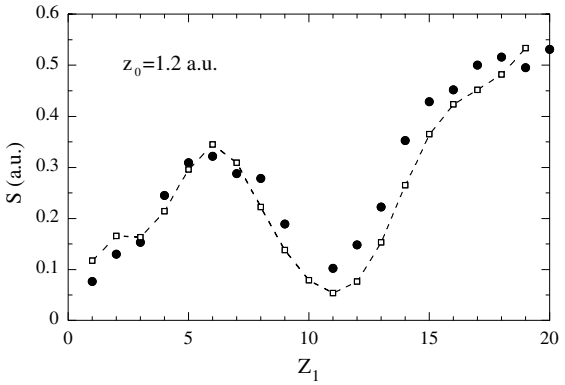

Fig. 5. Stopping power of ions with $v = 0.5$ a.u. as a function of the atomic number Z_1 at a distance $z_0 = 1.2$ a.u. from an Al(1 1 1) surface. Full circles denote the experimental data and open squares the results obtained for $r_s = 2.2$ a.u. with Eq. (9).

3.3. Charge state dependence of the energy loss of slow ion interacting with metal surfaces

Another problem of interest that has been successfully treated using the above described formalism is the study of the energy loss of slow multicharged ions in metals as a function of their initial charge state [44,45]. The interesting question that one has to answer is how preequilibrium of charge states does affect the energy loss of multicharged projectiles.

In an experiment performed by Winter et al. in the Humboldt University in Berlin, the mean energy loss of N ions after scattering from an Al(1 1 1) surface under a grazing angle of incidence $\phi = 0.7°$ was measured [44,45]. In Fig. 6 it is shown the mean energy loss as a function of the charge state q of the incident ions. Since, for a N^{q+} ion, the energy loss is constant for a variation of the angle of incidence [46], the analysis of the data is simplified. More precisely, the observed constancy of ΔE with variations of ϕ allows one to neglect effects on the energy loss by changing the trajectory [24]. In other words, the observed increase of the

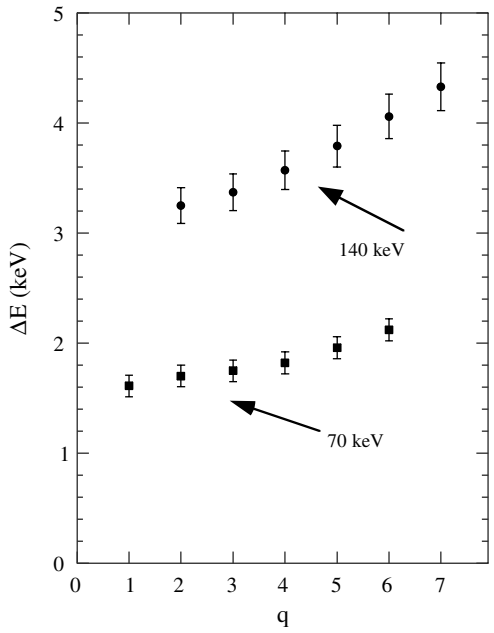

Fig. 6. Measured energy loss for 70 and 140 keV N^{q+} ions as a function of q the incident charge state of the projectiles after scattering from an Al(1 1 1) surface under a grazing angle of incidence $\phi = 0.7°$.

energy loss with the incident charge state can only be due to a corresponding enhancement of the stopping power with the charge state.

Nevertheless, the screening effects by conduction band electrons make the electronic stopping of atomic projectiles a complex problem. In this respect, one needs to incorporate the effect produced in the electronic stopping by the presence of inner-shell vacancies [47]. With this aim the formula described in Section 3.1 has to be generalized in order to study projectiles with vacancies in their bound states. This is done by using the KS orbitals in an approximate way as monoelectronic wave functions. Accordingly, one can fix the number n_v of empty orbitals when solving iteratively the KS equations [48].

Using this model one can calculate the stopping power (or accordingly the friction coefficient Q) as given by Eq. (9) for different configurations of inner-shell vacancies. In Fig. 7 results are presented for the friction coefficient Q of N ions travelling through an Al metal as a function of n_v. As explained, Q is calculated in terms of the transport

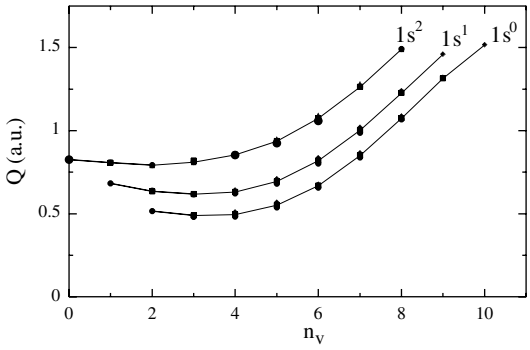

Fig. 7. Friction coefficient Q as a function of the total number of inner-shell vacancies n_v for $Z_1 = 7$ in an electron gas with $r_s = 2$ a.u. The curve $1s^2$ is obtained for a filled K-shell, $1s^1$ for one electron in the K-shell and $1s^0$ for an empty K-shell. The solid circles represent the $2s^2$, the open circles represent $2s^1$, and the solid triangles represent $2s^0$ configurations of the L-shell. The solid lines are drawn to guide the eye.

cross-section at the Fermi level, obtained for electron scattering at the potential induced by the projectile. This potential, is calculated within DFT, for different inner-shell configurations. It is observed that for a given K-shell occupancy the stopping is affected in an appreciable manner by the number of L-shell electrons: Q increases as the number of L-shell vacancies increases for $n_v > 3$, whereas it is essentially constant for $n_v \leqslant 3$. The L-subshell distribution of electrons has practically no influence on Q. However, Q decreases as the number of vacancies in the K-shell increases when n_v is low, and is almost constant when n_v is high. This opposite behaviour of Q with the number of vacancies in the K- and L-shells is related to the degree of spatial localization of the different orbitals (see [44] for details).

The three different sets of data in Fig. 7 can be used to understand the neutralization/relaxation sequences for incident N^{5+}, N^{6+} and N^{7+} ions. In case of ions without K-shell vacancies one should use the curve labeled $1s^2$. For instance, for N^{5+} one should start from the point that corresponds to the fully unoccupied L-shell ($n_v = 8$), with the highest value of the stopping power. Along its incoming trajectory the number of electrons in the L-shell will increase due to LVV Auger processes, and the value of the stopping will be reduced. Comparing to N^{5+}, the main difference

for N^{6+} and N^{7+} ions is a longer neutralization sequence due to the presence of inner-shell vacancies. The filling of the K-shell vacancy is interpreted as a transition to the adjacent curve in the figure towards smaller n_v value for a KVV process and towards a larger value of n_v for a KLL process. Therefore, the enhanced energy loss for higher charge states of incident ions observed in Fig. 6, is attributed to the enhanced friction coefficients Q obtained in the calculation for ions with several L-shell vacancies. Whereas the calculation shows an enhancement of electronic stopping for projectiles with empty L-shells (N^{5+}, N^{6+} and N^{7+} ions) over ground state ions by a factor of 2, the experimental energy loss increases with charge only by up to 35%. This finding can be considered as an indication of the fact that the lifetime of L-shell vacancies is shorter than the interaction time of the ions with the surface. From these observations one can infer a lifetime of the L-shell vacancies of the order of 2 fs, which is consistent with theoretical calculations [49–51].

The study shows that the charge state dependence of the energy loss of slow multicharged ions traveling through the electron gas of a metal is the outcome of a complex situation, where both the different screening (and the resulting different stopping powers) and the lifetimes of the excitation states of the ions play a role. For N^{q+} ions it is found that the experimentally observed increase of the energy loss with the charge state of the ion can be explained by a larger stopping power of ions with vacancies in the L-shell and by a longer lifetime of the configurations with K-shell vacancies.

4. Final remarks and conclusions

In this work some recent developments in the energy loss of ions scattered off solid surfaces have been reviewed. In the weak-coupling regime ($Z_1/v \ll 1$) linear response theory allows one to calculate the distance dependent stopping power. In this respect, it has been shown that a linear approach with the SRM is a good approximation for obtaining the distance dependent stopping power $S(z)$ for high velocity projectiles. It has also been shown that for high velocity protons specularly reflected from Al(1 1 1) the experimental energy loss is reproduced if the energy lost in the excitation of the L-shell of the target atoms is taken into account.

In the strong-coupling regime ($Z_1/v \gg 1$), in which linear approaches are not valid, an approach developed for slow ions travelling through jellium based on DFT and a full phase-shift calculation of the cross-sections is successful in accounting for the value of the stopping power at short distances from the surface, where density nonuniformities are small. It is remarkable the excellent agreement obtained by this model for the measured Z_1 oscillations of the stopping power close to an Al surface. Since most of the energy loss of the slow ions takes place in the region close to the surface this model allows one to understand, for instance, the measured charge state dependence of the energy loss.

Acknowledgements

I am indebted to P.M. Echenique, H. Winter, A. Arnau, V.M. Silkin, M. Alducin and F.J. García de Abajo, for crucial contributions in some of the presented works. Partial support by the Eusko Jaurlaritza, Gipuzkoako Foru Aldundia, Euskal Herriko Unibertsitatea (project number: 9/UPV00206.215-13639/2001) and by the Spanish MCyT (project number: BFM-2001-0076) is acknowledged.

References

[1] H. Winter, Phys. Rep. 367 (2002) 387.
[2] M. Alducin, J.I. Juaristi, R. Díez Muiño, A. Arnau, Recent Res. Dev. Phys. 4 (2003) 97.
[3] M. Alducin, J.I. Juaristi, Adv. Quantum Chem. 45 (2004) 223.
[4] J.I. Juaristi, F.J. García de Abajo, Nucl. Instr. and Meth. B 90 (1994) 252.
[5] J.I. Juaristi, F.J. García de Abajo, P.M. Echenique, Phys. Rev. B 53 (1996) 13839.
[6] M.A. Cazalilla, F.J. García de Abajo, Nucl. Instr. and Meth. B 125 (1997) 106.
[7] M.S. Gravielle, Phys. Rev. A 58 (1998) 4622.
[8] Y.H. Song, Y.N. Wang, Nucl. Instr. and Meth. B 153 (1999) 186.

[9] M.A. Cazalilla, J.I. Juaristi, Nucl. Instr. and Meth. B 157 (1999) 104.
[10] Y.H. Song, Y.N. Wang, Z.L. Miskovic, Phys. Rev. A 63 (2001) 052902.
[11] A. García-Lekue, J.M. Pitarke, Phys. Rev. B 64 (2001) 035423.
[12] M.S. Gravielle, J.E. Miraglia, Phys. Rev. A 65 (2002) 022901.
[13] P.M. Echenique, F.J. García de Abajo, V.H. Ponce, M.E. Uranga, Nucl. Instr. and Meth. B 96 (1995) 583.
[14] A.G. Eguiluz, Phys. Rev. Lett. 51 (1983) 1907.
[15] A.G. Eguiluz, Phys. Rev. B 31 (1985) 3303.
[16] R.H. Ritchie, A.L. Marusak, Surf. Sci. 4 (1966) 234.
[17] D. Wagner, Z. Naturforsch. A 21 (1966) 634.
[18] J. Lindhard, K. Dan, Vidensk. Selsk. Mat. Fys. Edd. 28 (8) (1954) 1.
[19] M. Alducin, V.M. Silkin, J.I. Juaristi, E.V. Chulkov, Nucl. Instr. and Meth. B 193 (2002) 585.
[20] M. Alducin, V.M. Silkin, J.I. Juaristi, E.V. Chulkov, Phys. Rev. A 67 (2003) 032903.
[21] H. Winter, M. Wilke, M. Bergomaz, Nucl. Instr. and Meth. B 125 (1997) 124.
[22] R. McCarroll, A. Salin, C.R. Acad. Sci. Paris 263B (1966) 329.
[23] J.F. Ziegler, J.P. Biersack, U. Littmark, in: J.F. Ziegler (Ed.), Stopping and Range of Ions in Matter, Vol. 1, Pergamon, New York, 1985.
[24] K. Kimura, M. Hasegawa, M. Mannami, Phys. Rev. B 36 (1987) 7.
[25] E. Zaremba, L.M. Sander, H.B. Shore, J.H. Rose, J. Phys. F 7 (1977) 1763.
[26] C.O. Almbladh, U. von Barth, Z.D. Popovic, M.J. Stott, Phys. Rev. B 14 (1976) 2250.
[27] P.M. Echenique, F. Flores, R.H. Ritchie, in: H. Ehrenreich, D. Turnbull (Eds.), Solid State Physics: Advances in Research and Applications, Vol. 43, Academic Press, New York, 1990, p. 229.
[28] P.M. Echenique, I. Nagy, A. Arnau, Int. J. Quantum Chem. 23 (1989) 521.
[29] I. Nagy, B. Apagyi, K. Ladányi, Phys. Rev. A 42 (1990) 1806.
[30] K. Ladányi, I. Nagy, B. Apagyi, Phys. Rev. A 45 (1992) 2989.
[31] P.M. Echenique, R.M. Nieminen, R.H. Ritchie, Solid State Commun. 37 (1981) 779.
[32] P.M. Echenique, R.M. Nieminen, J.C. Ashley, R.H. Ritchie, Phys. Rev. A 33 (1986) 897.
[33] I. Nagy, A. Arnau, P.M. Echenique, Phys. Rev. B 40 (1989) 11983.
[34] I. Nagy, A. Arnau, P.M. Echenique, Phys. Rev. A 40 (1989) 987.
[35] E. Zaremba, A. Arnau, P.M. Echenique, Nucl. Instr. and Meth. B 96 (1995) 619.
[36] A. Salin, A. Arnau, P.M. Echenique, E. Zaremba, Phys. Rev. B 59 (1999) 2537.
[37] J.H. Omrod, H.E. Duckworth, Can. J. Phys. C 41 (1963) 1424.
[38] J.H. Omrod, J.R. Macdonald, H.E. Duckword, Can. J. Phys. C 43 (1965) 275.
[39] F.H. Eisen, Can. J. Phys. C 46 (1968) 561.
[40] J. Böttiger, F. Bason, Radiat. Eff. 2 (1969) 105.
[41] G. Högberg, Phys. Status Solidi B 46 (1971) 829.
[42] D. Ward, H.R. Andrews, I.V. Mitchell, W.N. Lennard, R.E. Walker, N. Rud, Can. J. Phys. C 57 (1979) 645.
[43] H. Winter, J.I. Juaristi, I. Nagy, A. Arnau, P.M. Echenique, Phys. Rev. B 67 (2003) 245401.
[44] J.I. Juaristi, A. Arnau, P.M. Echenique, C. Auth, H. Winter, Phys. Rev. Lett. 82 (1999) 1048.
[45] J.I. Juaristi, A. Arnau, P.M. Echenique, C. Auth, H. Winter, Nucl. Instr. and Meth. B 157 (1999) 87.
[46] H. Winter, C. Auth, A. Mertens, A. Kirste, M.J. Steiner, Europhys. Lett. 41 (1998) 437.
[47] J.I. Juaristi, A. Arnau, Nucl. Instr. and Meth. B 115 (1996) 173.
[48] A. Arnau, P.A. Zeijlmans van Emmichoven, J.I. Juaristi, E. Zaremba, Nucl. Instr. and Meth. B 100 (1995) 279.
[49] R. Díez Muiño, A. Salin, N. Stolterfoht, A. Arnau, P.M. Echenique, Phys. Rev. A 57 (1998) 1126.
[50] R. Díez Muiño, N. Stolterfoht, A. Arnau, A. Salin, P.M. Echenique, Phys. Rev. Lett. 76 (1996) 4636.
[51] N. Vaeck, J.E. Hansen, J. Phys. B 25 (1992) 883.